JOURNAL OF VIROLOGY, Nov. 1998, p. 8517–8524 Vol. 72, No. 11
0022-538X/98/$04.00+0

Coronavirus Transcription Early in Infection

SUNGWHAN AN, AKIHIKO MAEDA, AND SHINJI MAKINO*

Department of Microbiology and Institute for Cellular and Molecular Biology, The University of Texas at Austin, Austin, Texas 78712-1095

Received 18 May 1998/Accepted 24 July 1998

We studied the accumulation kinetics of murine coronavirus mouse hepatitis virus (MHV) RNAs early in infection by using cloned MHV defective interfering (DI) RNA that contained an intergenic sequence from which subgenomic DI RNA is synthesized in MHV-infected cells. Genomic DI RNA and subgenomic DI RNA accumulated at a constant ratio from 3 to 11 h postinfection (p.i.) in the cells infected with MHV-containing DI particles. Earlier, at 1 h p.i., this ratio was not constant; only genomic DI RNA accumulated, indicating that MHV RNA replication, but not MHV RNA transcription, was active during the first hour of MHV infection. Negative-strand genomic DI RNA and negative-strand subgenomic DI RNA were first detectable at 1 and 3 h p.i., respectively, and the amounts of both RNAs increased gradually until 6 h p.i. These data showed that at 2 h p.i., subgenomic DI RNA was undergoing synthesis in the cells in which negative-strand subgenomic DI RNA was undetectable. These data, therefore, signify that negative-strand genomic DI RNA, but not negative-strand subgenomic DI RNA, was an active template for subgenomic DI RNA synthesis early in infection.

Coronavirus, an enveloped virus containing a large positive-sense single-strand RNA, expresses its genes by producing subgenomic mRNAs. Cells infected with coronavirus produce six to eight species of virus-specific mRNAs that make up a 3′-coterminal nested-set structure and that are expressed in different quantities (9, 11). The 5′ end of each coronavirus genomic RNA and subgenomic mRNA starts with a leader sequence that is approximately 60 to 90 nucleotides (nt) long (9, 10, 27). The leader RNA joins to the body of the subgenomic RNA at the intergenic sequence (10, 17, 26, 27). Coronavirus mRNAs are detectable within a few hours postinfection (p.i.) by metabolic labeling and Northern blot analysis of coronavirus-specific intracellular RNAs (11, 28). Once coronavirus mRNA accumulates to a detectable level, thereafter relative molar ratios of the different mRNAs are roughly constant (11, 25, 28); the only reported exception is an enhanced synthesis of the genomic-size RNA late in bovine coronavirus infection (8). The amounts of coronavirus mRNAs are low early in infection, and whether or not the relative molar ratios of these mRNAs are constant during this stage of infection is unknown.

Coronavirus is a typical positive-strand RNA virus, so coronavirus RNA synthesis involves the synthesis of negative-strand RNAs that are used as template RNAs for positive-strand RNA synthesis. Coronavirus negative-strand RNAs represent only 1 to 2% of the total intracellular virus-specific RNAs (19, 21). In addition to negative-strand RNA of genomic size, negative-strand subgenomic RNAs, each of which corresponds to a subgenomic mRNA species, are produced in coronavirus-infected cells (6, 25). These negative-strand RNAs contain an antileader sequence at the 3′ end and a poly(U) sequence at the 5′ end (24). The biological function of these negative-strand subgenomic coronavirus RNAs in coronavirus RNA synthesis has not been established; they may be active template RNAs for subgenomic mRNA synthesis (22, 23, 25), or they may be transcriptionally inactive, dead-end products (7). Northern blot analysis of negative-strand RNAs from transmissible gastroenteritis virus and bovine coronavirus showed that the relative molar ratios of the various subgenomic negative-strand RNAs are comparable to those of subgenomic mRNAs (25) late in infection. Kinetic studies of murine coronavirus mouse hepatitis virus (MHV) negative-strand RNA synthesis (including both genomic-size and subgenomic-size RNAs) showed that at 37°C negative-strand RNA synthesis is detectable at 3 h p.i., becomes maximal at 6 h p.i., and then declines (21). Using cloned MHV defective interfering (DI) RNA, which contains an inserted intergenic sequence to produce subgenomic DI RNA, Lin et al. showed that negative-strand DI RNAs (negative-strand genomic DI RNA and negative-strand subgenomic DI RNA were not distinguished in these experiments) are detected as early as 20 min after transfection of DI RNA into MHV-infected cells (12). The amounts of negative-strand DI RNAs reach a plateau at 1 h posttransfection and do not increase thereafter (12). This very rapid accumulation of negative-strand DI RNAs reported by Lin et al. (12) differs distinctly from kinetic characterizations of coronavirus negative-strand RNAs by others (21, 25). The kinetics of negative-strand genomic RNA and negative-strand subgenomic RNA accumulation in early infection is not known because of the very low level of coronavirus negative-strand RNA production early in infection.

We have investigated MHV RNA accumulation early in viral infection by characterizing MHV DI RNA that produces subgenomic DI RNA. We used MHV DI RNA for the following reasons. (i) Although the ratio of subgenomic DI RNA to genomic DI RNA is lower than the corresponding ratio of mRNA 7 to mRNA 1 (1, 14, 15), MHV DI RNA depends upon borrowing the MHV RNA synthesis mechanism for its own synthesis. Hence, the kinetics of MHV DI RNA synthesis most probably is the same or very similar to that of MHV mRNA synthesis. (ii) MHV DI RNA produces only one subgenomic DI RNA, which makes the characterization of this genomic DI RNA and its subgenomic DI RNA much simpler than that of MHV genomic RNA with its six to seven subgenomic mRNAs. (iii) DI RNA can be altered to carry non-MHV sequences, which we can specifically target for detection of MHV DI RNA synthesis via radiolabeled probes and oligonucleotide primers.

Our study indicated that the MHV RNA replication mech-

* Corresponding author. Mailing address: Department of Microbiology, The University of Texas at Austin, Austin, TX 78712-1095. Phone: (512) 471-6876. Fax: (512) 471-7088. E-mail: makino@mail.utexas.edu.

TABLE 1. Synthetic oligonucleotides used in this study

Oligonucleotide	Sequence[a] (5′–3′)
10401	AATCGCGTCCCTGATCTCAGCGGATTTCATCTGACTAATACTAC
10402	TATAAGAGTGATTGGCGTACTAATACTACAACACCACC
10124	AATCGCGTCCCTGATCTCAGCGG
10403	ATCCCATATCACCAGCTCAC
10066	TATAAGAGTGATTGGCGTCCG
10404	AAGC**TTAATACGACTCACTATAGGG**ATCCCATATCACCAGCTCAC
10319	AAGC**TTAATACGACTCACTATAGGG**TTTGCTTCATGGAAAACGGTGTAACAAGGGTGAACACTATCCCATATCACCAGCTCAC

[a] Boldface letters indicate a T7 promoter sequence; underlined nucleotides represent a 38-nt sequence that is not related to that of MHV RNA or MIGCAT RNA.

anism, but not the RNA transcription mechanism, was active very early in infection. Furthermore, we provide evidence that negative-strand genomic DI RNA, but not negative-strand subgenomic DI RNA, serves as a template for subgenomic DI RNA synthesis early during MHV infection.

MATERIALS AND METHODS

Viruses and cells. The plaque-cloned A59 strain of MHV (9) was used as a helper virus. Mouse DBT cells (5) were used for MHV growth and RNA transfection.

DNA construction. The synthetic oligonucleotides used in the present study are listed in Table 1. Plasmid MIGCAT was constructed by inserting a DNA fragment consisting of the 18-nt intergenic sequence from MHV genes 6 and 7 (5′-AAUCUAAUCUAAACUUUA-3′) and the 5′-most 0.3-kb region of the chloramphenicol acetyltransferase (CAT) gene into the large *Kpn*I-*Eco*RV fragment of MHV DI cDNA, PR6 (15). In the present study, the first nucleotide of the CAT sequence was defined as nt +1 (Fig. 1). Gel-purified PCR products corresponding to a part of the CAT sequence from nt +21 to +237 were used as a probe (DNA probe 1; Fig. 1). PCR products used to produce riboprobe 1 were made by incubating MIGCAT plasmid with two oligonucleotides. One is oligonucleotide 10124, which hybridizes with negative-strand MHV RNAs at nt −112 to −90 (Fig. 1); the other is oligonucleotide 10319, which contains the T7 promoter sequence, a 38 nt-long sequence that is related to neither the MHV nor the MIGCAT sequence, and a sequence corresponding to nt +278 to +297 of the positive-strand RNA. PCR products were made by incubating MIGCAT DNA with oligonucleotide 10401, which consists of sequences from nt −112 to −92 and from nt +8 to +28, and oligonucleotide 10401, which consists of sequences from nt −112 to −92 and from nt +8 to +28, and oligonucleotide 10404, which contains the T7 promoter sequence and a sequence from nt +278 to +297 (Fig. 1). Gel-purified PCR products were used as a source for the template DNA for the synthesis of competitor A RNA in vitro. A similar procedure was used for construction of DNA containing competitor B, except that oligonucleotide 10402, which consists of a part of the leader sequence (from nt −78 to −58 in the subgenomic MIGCAT RNA) and the sequence from nt +18 to +37, was used in place of oligonucleotide 10401.

RNA transcription and transfection. MIGCAT DI RNA transcripts were synthesized in vitro with T7 polymerase (16) and then transfected into MHV A59-infected DBT cells (3) by using a lipofection procedure, as described previously (15). Virus released into the culture supernatant was collected 15 h after RNA transfection and was subsequently passaged twice on DBT cells to amplify the DI particles containing MIGCAT DI RNA (MIGCAT DI particles). This virus preparation was designated P2.

Virus inoculation and preparation of virus-specific intracellular RNA. DBT cells were infected with the P2 sample at a multiplicity of infection of 5 and incubated at 0°C for 30 min for virus adsorption. Unadsorbed virions were removed by washing the cells once with chilled minimum essential medium

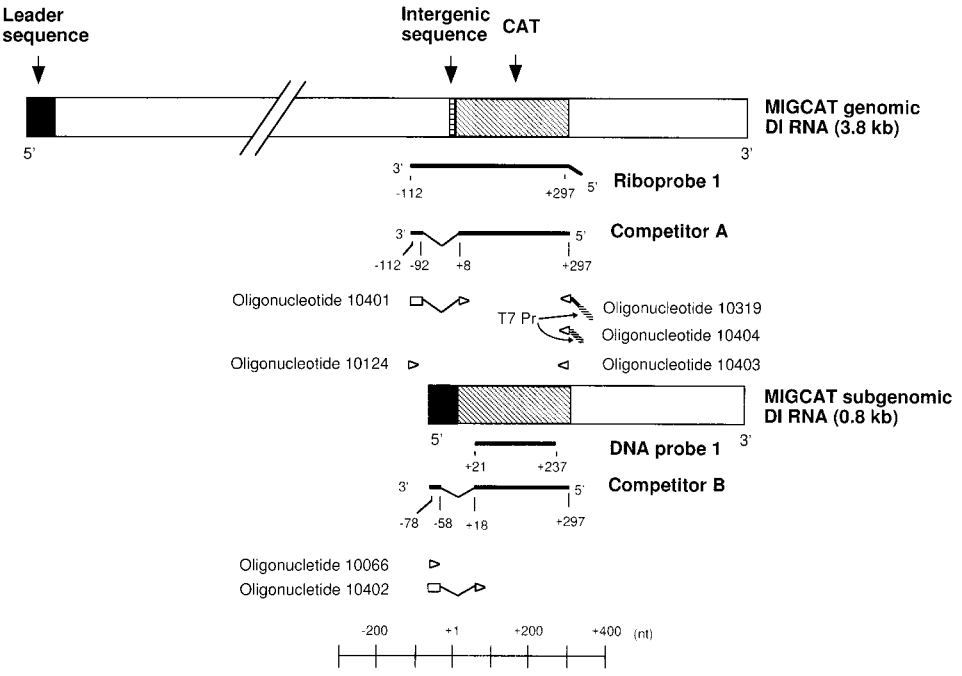

FIG. 1. Schematic diagram of the structure of genomic MIGCAT RNA and subgenomic MIGCAT RNA. The locations of leader sequences, an intergenic sequence, and CAT sequences are indicated. Oligonucleotides used for RT-PCR and the preparation of riboprobe 1, competitor A, and competitor B are shown by open arrowheads. T7 Pr, the T7 promoter sequence present at the 5′ ends of oligonucleotides 10319 and 10404. The short boldface line between the open arrowhead and the T7 promoter sequence in oligonucleotide 10319 represents a unique sequence that does not hybridize with either MIGCAT or MHV RNA sequences. Structures of probes used in the present study are also shown; the positions of riboprobe 1 and competitor A relative to genomic MIGCAT RNA and the positions of DNA probe 1 and competitor B relative to subgenomic MIGCAT RNA are shown. Riboprobe 1, competitor A, and competitor B are complementary to positive-strand MIGCAT-specific RNAs. Nucleotide numbers shown for these probes start from the beginning of the CAT sequence.

(MEM) and once with prewarmed MEM. Immediately after the washing of the cells total intracellular RNAs were extracted by using the Totally RNA kit (Ambion). This sample was denoted the 0-h p.i. sample. Other virus-infected cells were cultured at 37°C, and total intracellular RNAs were extracted at various times p.i.

Northern (RNA) blotting. Northern blot analysis using ^{32}P-labeled random-primed DNA probe 1 (approximately 2×10^9 cpm/μg) (Fig. 1) was performed as previously described (20).

RNase protection assay. The RNase protection assay was carried out as described by Zinn et al. (32) with some modification. Briefly, a ^{32}P-labeled 440-nt RNA probe, riboprobe 1, was prepared by using in vitro transcription of the riboprobe 1-specific PCR products (see above). The 5′-end 38 nt of riboprobe 1 were not related to nucleotides from either MIGCAT or MHV, while the rest of the probe was complementary to genomic MIGCAT RNA from nt −112 to +297 (Fig. 1). Intracellular RNAs extracted from 0 to 4 h p.i. were heat denatured at 90°C for 2 min and quickly chilled on ice. Heat-denatured RNA was incubated with ^{32}P-labeled riboprobe 1 in a 30-μl solution containing 80% formamide, 40 mM PIPES (piperazine-*N*,*N*′-bis(2-ethanesulfonic acid; pH 6.4), 400 mM NaCl, and 1 mM EDTA at 60°C. After 8 h of incubation, 300 μl of a solution containing 100 mM NaCl, 10 mM Tris-HCl (pH 7.5), 5 mM EDTA, 15 μg of RNase A per ml, and 1 μg of RNase T_1 per ml was added, and the mixture was incubated for 10 min at 15°C. The RNase reactions were terminated by adding 10 μl of 10% sodium dodecyl sulfate and 2 μl of 5-mg/ml proteinase K, followed by incubation at 37°C for 15 min, phenol extraction, and ethanol precipitation. Precipitated RNA was then applied to a 6% sequencing gel.

RT-PCR. To amplify negative-strand genomic MIGCAT RNA, the RNA sample was heated at 90°C for 2 min and quickly chilled on ice. Heat-denatured RNA was then incubated with oligonucleotide 10124 in 25 μl of avian myeloblastosis virus reverse transcriptase (RT) reaction buffer containing avian myeloblastosis virus RT for cDNA synthesis (Promega). Then, 1 μl of cDNA sample was mixed with 99 μl of PCR buffer (Promega) including oligonucleotide 10124 and oligonucleotide 10403, which hybridizes with the positive-strand MIGCAT sequence at nt +278 to +297 (Fig. 1). One piece of AmpliWax wax (Perkin-Elmer) was added to seal the sample mixture, and the PCR was started by incubating the sample mixture at 94°C for 2 min and then cooling it to 4°C. After this, *Taq* DNA polymerase was placed on top of the wax layer. The sample mixture was incubated at 72°C for 5 min once; at 94°C for 45 s, 60°C for 45 s, and at 72°C for 45 s for 34 cycles; and at 72°C for 5 min. For the detection of negative-strand subgenomic MIGCAT RNA, oligonucleotide 10066, which hybridizes with the antileader sequence of MIGCAT RNA at the first 21 nt from the 3′ end of the antileader sequence, was used in the place of oligonucleotide 10124 for cDNA synthesis and PCR. MIGCAT-specific RT-PCR products were detected by Southern blot analysis using ^{32}P-labeled DNA probe 1 as a probe (Fig. 1).

Competitive RT-PCR. Competitor A transcripts and competitor B transcripts were synthesized separately by T7 polymerase-mediated transcription in vitro, and the samples containing competitor A and competitor B were incubated with DNase I to digest DNA. The amounts of competitor A and competitor B were quantitated by using a spectrophotometer and by a visual inspection of RNA bands after agarose gel electrophoresis of the transcripts; 40-ng amounts of competitor A and competitor B were used as the undiluted samples. Total intracellular RNA extracted from MIGCAT-replicating cells (2×10^6 cells) was dissolved in 20 μl of water. To estimate negative-strand genomic MIGCAT RNA, 2 μl of intracellular RNA sample was mixed with oligonucleotide 10124 and with serially diluted in vitro-synthesized competitor A. After heat denaturation of RNAs, cDNA synthesis was performed. After cDNA synthesis, 1 μl of sample was mixed with 99 μl of PCR buffer containing oligonucleotides 10124 and 10403, and one piece of AmpliWax was added to the sample. After incubation of the sample mixture at 94°C for 2 min and subsequent cooling to 4°C, *Taq* DNA polymerase was added to the wax layer. The sample mixture was first heated to 94°C for 1 min and then immediately incubated at 94°C for 1 min, 63°C for 1 min, and 72°C for 1 min for 35 cycles. After the final cycle of incubation, the sample mixture was incubated at 72°C for 5 min. Aliquots of the sample were electrophoresed on 2% agarose gels, and RT-PCR products were detected by Southern blot analysis with ^{32}P-labeled DNA probe 1 as the probe. To estimate negative-strand subgenomic MIGCAT RNA, a similar procedure was used, except that competitor B was used as an internal control, oligonucleotide 10066 was used for cDNA synthesis, and a combination of oligonucleotides 10066 and 10403 was used for PCR.

RESULTS

Positive-strand MIGCAT RNA synthesis early in infection. We used MIGCAT DI particles to study MHV RNA accumulation kinetics. The 5′-most 3.1-kb region of MIGCAT RNA was made from the corresponding region of a cloned MHV strain JHM (MHV-JHM) DIssF DI RNA (18), PR6 (15). Downstream of the 3.1-kb region was an intergenic sequence and the 5′-most 0.3-kb region of the CAT gene. The 0.46-kb region closest to the 3′ end of MIGCAT RNA was derived from the corresponding region of the MHV-JHM genomic RNA (Fig. 1). We prepared a P2 virus sample that contained both helper MHV and MIGCAT DI particles by passaging twice the virus sample from the MHV-infected, MIGCAT RNA-transfected cells. To study the kinetics of MIGCAT RNA accumulation, DBT cells were inoculated with virus sample and then incubated at 0°C for 30 min for virus adsorption; virus adsorption, but not penetration, occurs during incubation at 0°C. Washing the cells with medium removed unadsorbed virus. Immediately after the washing, total intracellular RNA was extracted from the cells to determine the amount of MIGCAT RNA in the adsorbed virions. This RNA sample is referred to as the 0-h p.i. sample. The remaining virus-infected cells were then incubated at 37°C. Viral penetration is a synchronous event that begins immediately after incubation at 37°C. Intracellular RNAs were extracted hourly from 1 through 11 h p.i. Northern blot analysis using the ^{32}P-labeled CAT gene-specific probe, DNA probe 1, showed an accumulation of the 3.8-kb genomic MIGCAT RNA and the 0.8-kb subgenomic MIGCAT RNA as early as 4 h p.i. (Fig. 2A). The amount of MIGCAT-specific RNAs gradually increased from 4 to 8 h p.i., remained constant from 8 to 10 h p.i., and declined slightly at 11 h p.i. Because the majority of cells were still attached to the bottom of the plates at 11 h p.i., the slight reduction of MIGCAT-specific RNAs at 11 h p.i. was not due to the reduced number of cells in the sample preparation. Phosphorimager analysis of Northern blot membranes showed that the relative molar ratio of subgenomic MIGCAT RNA to genomic MIGCAT RNA was approximately 0.9 to 1.0 and remained constant from 5 to 11 h p.i. The relative molar ratios of MHV mRNAs were also constant during this period (11), so these data indicated that the accumulation of MIGCAT-specific RNAs faithfully reflected the accumulation of MHV mRNAs.

Northern blot analysis was not sensitive enough to detect minute amounts of MIGCAT-specific RNAs early in infection; therefore, we used an RNase protection assay to detect MIGCAT-specific RNA synthesis from 0 to 4 h p.i. In this assay we used a radiolabeled 440-nt RNA probe, riboprobe 1, whose 5′-end 38 nt were not related to nucleotides from either MIGCAT RNA or MHV RNA and whose remaining sequence was complementary to that part of the genomic MIGCAT RNA sequence extending from the end of the CAT sequence to 112 nt upstream of the CAT gene (Fig. 1). We anticipated that hybridization of radiolabeled riboprobe 1 with genomic MIGCAT RNA and subgenomic MIGCAT RNA followed by treatment of the hybrids with single-strand-specific RNases, should produce 0.41- and 0.32-kb labeled RNA bands, respectively. The RNase protection assay showed a gradual accumulation of genomic MIGCAT RNA from 1 to 4 h p.i. (Fig. 2B). No signal was detected in the sample extracted at 0 h p.i.; the RNA signal corresponding to genomic MIGCAT at 1 h p.i., therefore, represented genomic MIGCAT RNA synthesized during the first hour of infection and was not coming from input genomic MIGCAT RNA present in MIGCAT DI particles. We thought that the lack of a signal corresponding to subgenomic MIGCAT RNA at 1 h p.i., which we consistently saw in repeated experiments, was very interesting. An RNA signal corresponding to subgenomic MIGCAT RNA was first detectable at 2 h p.i. and then increased gradually from 2 to 4 h p.i. Phosphorimager scanning of the gels revealed that the ratio of the RNA signal corresponding to subgenomic MIGCAT RNA to that corresponding to genomic MIGCAT RNA was constant from 3 to 4 h p.i. The deduced relative molar ratio of subgenomic MIGCAT RNA to genomic MIGCAT RNA from 3 to 4 h p.i. was 0.9, which was similar to that of subgenomic

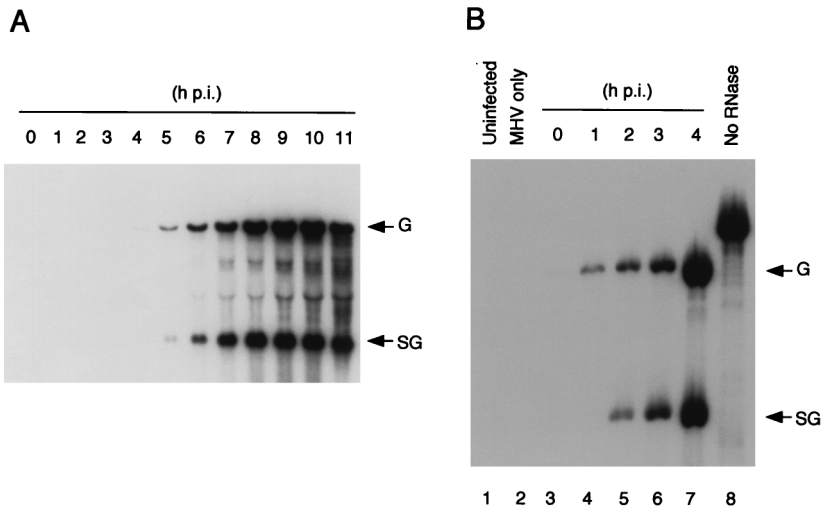

FIG. 2. Accumulation of positive-strand MIGCAT-specific RNAs. (A) Northern blot analysis of MIGCAT-specific RNAs. Total intracellular RNAs were extracted from MIGCAT DI particle-infected cells at the times shown above the gel. The sample at 0 h p.i. represents intracellular RNAs that were extracted immediately after 30 min of virus adsorption at 0°C. ^{32}P-labeled DNA probe 1 was used as a probe. (B) RNase protection assay of genomic MIGCAT RNA and subgenomic MIGCAT RNA. Heat-denatured intracellular RNA and radiolabeled riboprobe 1 (see Fig. 1) were hybridized and then treated with RNase A and RNase T_1. Riboprobe 1 fragments that were protected from RNase digestion were detected by separating the sample on 6% sequencing gels. Lanes 1 and 2 represent intracellular RNAs from non-MHV-infected and MHV-infected cells, respectively. Lane 8 is the same as lane 4, except that RNase treatment was omitted. G, genomic MIGCAT RNA; SG, subgenomic MIGCAT RNA.

MIGCAT RNA to genomic MIGCAT RNA from 5 to 11 h p.i. (Fig. 2A), demonstrating that the relative molar ratio of subgenomic MIGCAT RNA to genomic MIGCAT RNA was constant from 3 to 11 h p.i. The relative molar ratio of subgenomic MIGCAT RNA to genomic MIGCAT RNA at 2 h p.i. was about two-thirds of that from 3 to 11 h p.i. These data demonstrated that MIGCAT DI RNA replication, but not transcription, occurred during the first hour of infection, suggesting that RNA replication activity, but not RNA transcription activity, was active very early in MHV infection.

Negative-strand MIGCAT RNA synthesis early in infection. We next examined the kinetics of negative-strand MIGCAT RNA accumulation. We chose an RT-PCR procedure because Northern blot analysis using various ^{32}P-labeled riboprobes or ^{32}P-labeled oligonucleotide probes was not sensitive enough to detect negative-strand MIGCAT RNAs (data not shown). After heat denaturation of intracellular RNA extracted from MIGCAT-replicating cells, negative-strand genomic MIGCAT RNA-specific cDNA and negative-strand subgenomic MIGCAT RNA-specific cDNA were synthesized by using primer oligonucleotides 10124 and 10066, respectively (Fig. 1). The RT was inactivated by heating, and oligonucleotide pairs 10124 and 10403 and 10066 and 10403 (Fig. 1) were used to generate negative-strand genomic MIGCAT RNA-specific PCR products and negative-strand subgenomic MIGCAT RNA-specific PCR products, respectively. Southern blot analysis of RT-PCR products by using ^{32}P-labeled DNA probe 1 indicated that negative-strand genomic MIGCAT RNA gradually accumulated from 1 to 6 h p.i., became constant from 6 to 10 h p.i., and then declined at 11 h p.i. (Fig. 3A). No signal was detectable in the RNA sample extracted at 0 h p.i. in repeated experiments, indicating that the PCR signal in the sample at 1 h p.i. indeed represented the newly synthesized negative-strand genomic MIGCAT RNA. To our surprise, the PCR products corresponding to negative-strand subgenomic MIGCAT RNA were not detectable in the RNA samples extracted from 0 to 2 h p.i. (Fig. 3B), even after longer exposure of the gels or changing PCR conditions (data not shown), demonstrating that negative-strand subgenomic MIGCAT RNA most probably was not produced or was produced in extremely minute amounts from 0 to 2 h p.i. Negative-strand subgenomic MIGCAT RNA-specific PCR products were consistently detected at 3 h p.i. The amount of the RT-PCR products of negative-strand subgenomic MIGCAT RNA increased from 3 to 5 h p.i., remained constant up to 10 h, and slightly decreased at 11 h p.i. No RT-PCR products corresponding to the negative-strand MIGCAT-specific RNAs were detected in MHV-infected cells and in non-MHV-infected cells, demonstrating that these RT-PCR products were specific for MIGCAT RNAs (Fig. 3A and B). RT-PCR with 100 times less or 10 times more cDNAs than were used for Fig. 3A and B showed that, in both cases, the amounts of negative-strand MIGCAT RNA-specific RT-PCR products were constant from 6 to 10 h p.i. (data not shown). RT-PCR with 100 times less cDNA produced fewer products than the RT-PCR shown in Fig. 3A and B; that with 10 times more cDNA produced more products. Furthermore, when PCR was performed with positive-strand MIGCAT RNA-specific cDNAs, under the same PCR conditions, the amounts of PCR products were significantly higher than the amounts of RT-PCR products shown in Fig. 3A and B (data not shown). These data demonstrated that sufficient amounts of primers and deoxynucleoside triphosphates were provided in the RT-PCR.

To estimate the difference in the amounts of negative-strand subgenomic MIGCAT RNA at 3 h p.i. and putative negative-strand subgenomic MIGCAT RNA, which might be present at 2 h p.i., intracellular RNA extracted from MIGCAT DI particle-infected cells at 3 h p.i. was diluted by 10-, 25-, or 100-fold and mixed with a constant amount of intracellular RNAs that were extracted from MHV-infected cells at 3 h p.i.; intracellular RNA was added to maintain a constant amount of helper virus-derived RNAs in each diluted sample. An undiluted intracellular RNA sample that was extracted from MIGCAT DI particle-infected cells at 3 h p.i. served as a control. RT-PCR of these samples readily demonstrated the presence of negative-strand subgenomic MIGCAT RNA in 10-fold dilutions of the

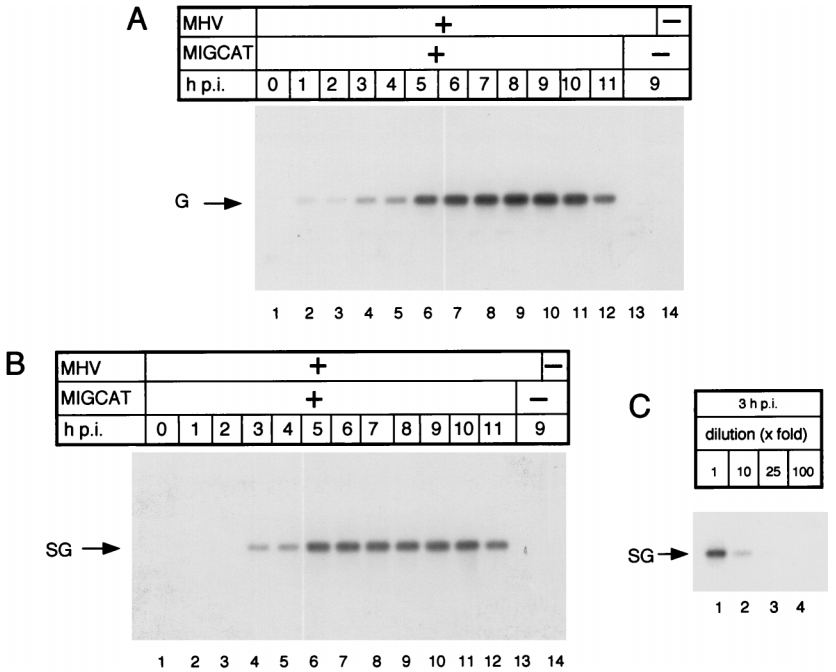

FIG. 3. Accumulation of negative-strand MIGCAT-specific RNAs. (A) Southern blot analysis of RT-PCR of negative-strand genomic MIGCAT RNA. Total intracellular RNAs were extracted from MIGCAT DI particle-infected cells at the times shown above the gel. Oligonucleotide 10124 was used for cDNA synthesis, and PCR amplification was performed by using oligonucleotides 10124 and 10403. PCR products were separated by agarose gel electrophoresis, and Southern blot analysis was performed by using ^{32}P-labeled CAT-specific probe DNA probe 1. For lane 13, RNA was extracted at 9 h p.i. from MHV-infected cells that did not contain MIGCAT DI RNA; for lane 14, RNA was extracted at 9 h p.i. from mock-infected cells. G, negative-strand genomic MIGCAT RNA-specific PCR products. (B) Southern blot analysis of RT-PCR of negative-strand subgenomic MIGCAT RNA. Total intracellular RNAs were extracted from MIGCAT DI particle-infected cells at the times shown above the gel. Oligonucleotide 10066 was used for cDNA synthesis, and PCR amplification was performed by using oligonucleotides 10066 and 10403. PCR products were separated by agarose gel electrophoresis, and Southern blot analysis was performed by using ^{32}P-labeled DNA probe 1. For lane 13, RNA was extracted at 9 h p.i. from MHV-infected cells that did not contain MIGCAT DI RNA; from lane 14, RNA was extracted at 9 h p.i. from mock-infected cells. SG, negative-strand subgenomic MIGCAT RNA-specific PCR products. (C) Southern blot analysis of RT-PCR of negative-strand subgenomic MIGCAT RNA with serial dilutions. Total intracellular RNAs were extracted from MIGCAT DI particle-infected cells at 3 h p.i. Total intracellular RNA was diluted 10-, 25-, or 100-fold and mixed with a constant amount of intracellular RNA extracted from MHV-infected cells at 3 h p.i. Oligonucleotide 10066 was used for cDNA synthesis, and PCR amplification was performed by using oligonucleotides 10066 and 10403. PCR products were separated by agarose gel electrophoresis, and Southern blot analysis was performed by using ^{32}P-labeled DNA probe 1. SG, negative-strand subgenomic MIGCAT RNA-specific PCR products.

sample (Fig. 3C). After extended exposure of the gel, negative-strand subgenomic MIGCAT RNA-specific RT-PCR products were also visible in the sample that was diluted 25-fold. We could not detect negative-strand subgenomic MIGCAT RNA-specific RT-PCR products at 2 h p.i. after long exposure of the gels in repeated experiments (Fig. 3B). As a result we feel that the amount of putative negative-strand subgenomic MIGCAT RNA at 2 h p.i., if any such RNA existed, was at least 25 times less than the amount of negative-strand subgenomic MIGCAT RNA at 3 h p.i.

Quantitative analysis of negative-strand MIGCAT RNAs early in infection. Because different sets of primers were used for PCR to amplify negative-strand genomic MIGCAT RNA and negative-strand subgenomic MIGCAT RNA, we could not directly compare the amounts of these RNAs in the above experiments. For comparing the amounts of negative-strand subgenomic MIGCAT RNA and negative-strand genomic MIGCAT RNAs early in infection, we used competitive RT-PCR. In competitive RT-PCR, a sample containing an unknown amount of the RNA of interest is added to serial dilutions of a known amount of a competitor RNA fragment that differs from the RNA of interest by having a small internal deletion. A primer which specifically binds to both the RNAs is used for cDNA synthesis, and a pair of primers is used to coamplify both RNAs. The ratio of the amount of PCR products of the RNA of interest to that of the competitor RNA should remain constant through the amplification, and the results should not be dependent on cycle number or on the concentrations of primers or deoxynucleoside triphosphates (4). At the point where the amounts of PCR products of the RNA of interest and of the competitor are equal, the starting concentration of the RNA of interest prior to PCR is equal to the known starting concentration of the competitor; in this way the amount of the RNA of interest can be easily estimated.

To estimate the amount of negative-strand genomic MIGCAT RNA, intracellular RNAs extracted from MIGCAT DI RNA-replicating cells were mixed with serially diluted known amounts of an in vitro-synthesized RNA transcript, competitor A, which contains a sequence corresponding to negative-strand genomic MIGCAT RNA with an internal deletion of 117 nt (Fig. 1). Oligonucleotide 10124 was used for cDNA synthesis and a pair of oligonucleotides, 10124 and 10403, was used for coamplification. For quantitation of negative-strand subgenomic MIGCAT RNA, serial dilutions of a known quantity of competitor B, which contains a sequence corresponding to the negative-strand subgenomic MIGCAT RNA with an internal deletion of 75 nt, were mixed with the intracellular RNA samples (Fig. 1). Oligonucleotide 10066 was used for cDNA synthesis, and oligonucleotides 10066 and 10403 were used for PCR. Equal amounts of competitor A and competitor B were prepared, diluted serially, and individually added with the same intracellular RNA sample prior to cDNA synthesis. Competitive RT-PCR showed that the amounts of RT-PCR products of negative-strand genomic MIGCAT RNA at 2 and

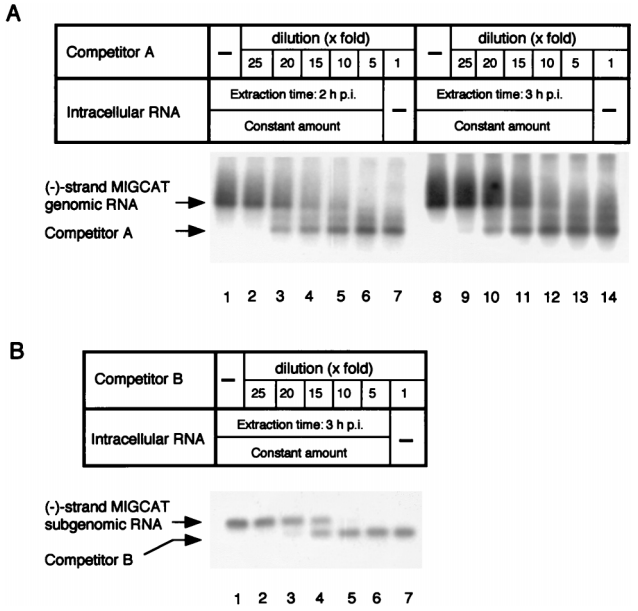

FIG. 4. Comparative RT-PCR of negative-strand MIGCAT-specific RNAs. (A) Total intracellar RNAs that were extracted from MIGCAT DI particle-infected cells at 2 (lanes 1 to 6) or 3 (lanes 8 to 13) h p.i. were mixed with serially diluted competitor A RNA. RT-PCR was performed to coamplify negative-strand genomic MIGCAT RNA and competitor A RNA. The accumulation of RT-PCR products was demonstrated by Southern blot analysis using ^{32}P-labeled DNA probe 1. Lanes 1 and 8 lack competitor A RNA, while lanes 7 and 14 lack intracellular RNA. (B) Total intracellular RNAs that were extracted from MIGCAT DI particle-infected cells at 3 h p.i. were mixed with serially diluted competitor B RNA. RT-PCR was performed to coamplify negative-strand subgenomic MIGCAT RNA and competitor B RNA. The accumulation of RT-PCR products was demonstrated by Southern blot analysis using ^{32}P-labeled DNA probe 1. Lane 1 and lane 7 lack competitor B RNA and intracellular RNA, respectively. The amounts of competitor A and competitor B RNA in the undiluted samples in panel A (lanes 7 and 14) and panel B (lane 7) were identical.

3 h p.i. were roughly equivalent to the amount of RT-PCR products of competitor A, which was diluted initially about 15- to 20-fold (Fig. 4A). These data indicated that there was no efficient accumulation of negative-strand genomic MIGCAT RNA from 2 to 3 h p.i. Increased RT-PCR signal from negative-strand genomic MIGCAT RNA from 2 to 3 h p.i., shown in Fig. 3A, probably did not reflect an actual change in the amount of negative-strand genomic MIGCAT RNA; small differences in each RT-PCR affected the amount of RT-PCR products. The amount of genomic MIGCAT RNA increased by approximately threefold during the same period of time (Fig. 2B), indicating that MHV positive-strand genomic RNA synthesis was more active than negative-strand genomic RNA synthesis at 3 h p.i. The amount of negative-strand subgenomic MIGCAT RNA at 3 h p.i. was approximately the same as the amount of RT-PCR products of competitor B when competitor B was diluted about 15-fold (Fig. 4B). In other experiments the amount of PCR products of negative-strand subgenomic MIGCAT RNA at 3 h p.i. was similar to the amount of RT-PCR products of competitor B when competitor B was diluted 20-fold (data not shown). The amounts of undiluted competitor A and undiluted competitor B at 3 h p.i. were the same, and the amounts of negative-strand genomic MIGCAT RNA and negative-strand subgenomic MIGCAT RNA were roughly the same. At 3 h p.i., the amount of genomic MIGCAT RNA was also similar to that of subgenomic MIGCAT RNA (Fig. 2B), demonstrating that the relative molar ratio of genomic MIGCAT RNA to subgenomic MIGCAT RNA was similar to that of negative-strand genomic MIGCAT RNA to negative-strand subgenomic MIGCAT RNA at 3 h p.i. The amounts of negative-strand genomic MIGCAT RNA at 2 and 3 h p.i. and that of negative-strand subgenomic MIGCAT RNA at 3 h p.i. were similar (Fig. 4). The amount of subgenomic MIGCAT RNA at 2 h p.i. was approximately two-thirds that of genomic MIGCAT RNA (Fig. 2B), whereas negative-strand subgenomic MIGCAT RNA was not detected at 2 h p.i. (Fig. 3B). If negative-strand subgenomic MIGCAT RNA existed at 2 h p.i., its amount appeared to be at least 25 times less than that at 3 h p.i. (Fig. 3C). These data demonstrated that at 2 h p.i., the ratio of the amount of subgenomic MIGCAT RNA synthesized in cells to the amount of newly synthesized genomic MIGCAT RNA was about two-thirds, while the amount of putative negative-strand subgenomic MIGCAT RNA was at least 25 times less than that of negative-strand genomic MIGCAT RNA. Thus, our data strongly indicate that at 2 h p.i., subgenomic MIGCAT RNA was synthesized from negative-strand genomic MIGCAT RNA, but not from negative-strand subgenomic MIGCAT RNA.

DISCUSSION

Presence of MHV RNA replication activity, but not transcription activity, immediately after infection. We demonstrated that genomic MIGCAT RNA was synthesized at 1 h p.i., while subgenomic MIGCAT RNA was not (Fig. 2B). Assuming that MIGCAT RNA synthesis reflected the MHV RNA synthesis mechanism, our data indicate that MHV genomic RNA replication, not subgenomic RNA transcription, was active within the first hour of MHV infection. The absence of coronavirus RNA transcription activity very early in infection has not been described previously. Our data also suggested that the mechanism used for coronavirus RNA replication and that used for transcription are not identical. Similarly, a recent study suggested that the arterivirus equine arteritis virus, which is closely related to coronavirus, has different requirements for genome replication and transcription (29).

We do not know how MHV transcription is activated between the first and second hours p.i. RNA replication activity during the first hour of infection probably increases the amount of genomic-size mRNA 1, which encodes MHV gene 1 proteins which are believed to be essential for MHV RNA synthesis. Increased amounts of mRNA 1 probably result in an increased concentration of MHV gene 1 proteins. A higher concentration of gene 1 proteins at 2 h p.i. may facilitate the change in relative molar ratios among MHV gene 1 proteins; this change may be important for the activation of MHV RNA transcription. The change in the relative molar ratio of particular gene 1 proteins may be mediated by the efficiency of *trans* cleavage of the precursor gene 1 proteins by virus proteinases (2, 13, 31), since the efficiency of *trans* cleavage is likely to be increased when the concentration of substrate is increased.

MHV RNA replication activity appears to be a continuous activity that begins immediately after infection. How is replication maintained after transcription begins? One possibility is that MHV transcription activity may be used for both genomic RNA replication and subgenomic mRNA transcription after 1 h p.i. Another possibility is that RNA replication and RNA transcription may take place at different sites in the cells according to different distributions of gene 1 proteins; RNA replication and RNA transcription may use different combinations of gene 1 proteins. Also, accumulation of N protein, which occurs after activation of transcription activity, may involve regulation of RNA replication and transcription activities.

Accumulation kinetics of negative-strand MIGCAT RNAs. RT-PCR of MIGCAT negative-strand RNAs showed that negative-strand genomic MIGCAT RNA gradually accumulated from 1 to 6 h p.i. and that negative-strand subgenomic MIGCAT RNA accumulated from 3 to 6 h p.i. From 6 to 10 h p.i., the amounts of PCR products of both negative-strand MIGCAT RNAs were roughly constant; these amounts then declined at 11 h p.i. (Fig. 3). The gradual accumulation of MIGCAT negative-strand RNA early in infection and the constant amount of MIGCAT negative-strand RNAs later in infection constituted a pattern that was similar to the accumulation pattern of transmissible gastroenteritis virus negative-strand RNAs demonstrated by Northern blot analysis (25). Sawicki and Sawicki showed that MHV negative-strand RNA synthesis activity is detectable at 3 h p.i. and that the kinetics of negative-strand RNA increases up to 6 h p.i. and then declines to about 20% of the maximum rate by about 8 to 9 h p.i. (21). In their study, hybrids of RNase A-treated radiolabeled intracellular MHV RNA and an excess amount of nonradiolabeled MHV genomic RNA were treated with RNase A and RNase-resistant signals were considered to be negative-strand RNAs (21). Their study and our present study both showed that MHV negative-strand RNAs do not accumulate quickly in MHV-infected cells. MHV negative-strand RNA synthesis early in infection was previously characterized by Lin et al. (12). In their study, in vitro-synthesized MHV DI RNA was transfected into MHV-infected cells and the combined accumulation of negative-strand genomic DI RNA and negative-strand subgenomic DI RNA was estimated by a RNase protection assay. They showed very rapid negative-strand RNA accumulation and concluded that the amount of negative-strand RNAs was constant from 1 h posttransfection onward. It is not clear why the accumulation kinetics of negative-strand MHV DI RNAs shown in the present study is distinctly different from that of Lin et al. One of the major differences between their study and ours was that MIGCAT DI particles were used to infect and thereby initiate RNA synthesis in our study, while an RNA transfection procedure was used to introduce MHV DI RNA in their study (12). The introduction of a large amount of in vitro-synthesized DI RNA into MHV-infected cells might affect the results.

Synthesis of subgenomic MIGCAT RNA in the absence of negative-strand subgenomic MIGCAT RNA. The biological function of negative-strand subgenomic RNAs in coronavirus transcription has not been established. They may be active template RNAs for subgenomic mRNA transcription (22, 23, 25) or dead-end transcription products (7). In the present study we demonstrated that negative-strand subgenomic MIGCAT RNA was undetectable at 2 h p.i. (Fig. 3B), while subgenomic MIGCAT RNA synthesis was evident at the same time (Fig. 2B). The amount of subgenomic MIGCAT RNA was about two-thirds that of genomic MIGCAT RNA (Fig. 2B), whereas the amount of putative negative-strand subgenomic MIGCAT RNA, if any such RNA existed, was at least 25 times less than that of negative-strand genomic MIGCAT RNA (Fig. 3C). We interpret these data to mean that at 2 h p.i. negative-strand genomic MIGCAT RNA, but not negative-strand subgenomic MIGCAT RNA, was the template RNA for subgenomic MIGCAT RNA synthesis. A study of UV irradiation of MHV-infected cells at 2.5 or 3 h p.i. suggested that MHV mRNA synthesis requires the presence of a genomic-length RNA template early in the infection (30). Studies involving the superinfection of UV-irradiated MHV DI particles into MHV-infected cells at 4 h p.i. showed that negative-strand genomic DI RNA synthesis from input genomic DI RNA occurs prior to subgenomic-size DI RNA synthesis (14). Our present data were consistent with these published studies.

Is negative-strand genomic-size RNA an active template RNA for subgenomic mRNA transcription throughout MHV infection? Transfection of MHV DI RNA into MHV-infected cells at both 1 and 6 h p.i. results in the accumulation of genomic DI RNA and subgenomic DI RNA (7). The relative molar ratios of subgenomic DI RNA to genomic DI RNA at 9 h p.i. are the same for both transfection times. These data suggest that all of the activities necessary for each step of MHV RNA synthesis exist continuously through the first 6 h of MHV replication (7). The present study indicated that negative-strand genomic-size DI RNA was a template RNA for subgenomic DI RNA synthesis early in infection. Therefore, it is likely that subgenomic DI RNA is initially synthesized from negative-strand genomic-size DI RNA at the time that DI RNA is transfected into MHV-infected cells, i.e., at 6 h p.i. (7); an MHV transcription activity that uses negative-strand genomic RNA as a template for subgenomic mRNA synthesis probably is present throughout infection.

ACKNOWLEDGMENTS

This work was supported by Public Health Service grants AI29984 and AI32591 from the National Institutes of Health (to S.M.) and partially by a grant from the Research Fellowships of the Japanese Society for the Promotion of Science for Young Scientists (to A.M.).

REFERENCES

1. **An, S., and S. Makino.** 1998. Characterization of coronavirus cis-acting RNA elements and the transcription step affecting its transcription efficiency. Virology **243:**198–207.
2. **Bonilla, P. J., S. A. Hughes, and S. R. Weiss.** 1997. Characterization of a second cleavage site and demonstration of activity in *trans* by the papain-like proteinase of the murine coronavirus mouse hepatitis virus strain A59. J. Virol. **71:**900–909.
3. **Felgner, P. L., T. R. Gadek, M. Holm, R. Roman, H. W. Chan, M. Wenz, J. P. Northrop, G. M. Ringgold, and M. Danielson.** 1987. Lipofection: a highly efficient, lipid mediated DNA-transfection procedure. Proc. Natl. Acad. Sci. USA **84:**7413–7417.
4. **Gilliland, G., S. Perrin, K. Blanchard, and H. F. Bunn.** 1990. Analysis of cytokine mRNA and DNA: detection and quantitation by competitive polymerase chain reaction. Proc. Natl. Acad. Sci. USA **87:**2725–2729.
5. **Hirano, N., K. Fujiwara, S. Hino, and M. Matsumoto.** 1974. Replication and plaque formation of mouse hepatitis virus (MHV-2) in mouse cell line DBT culture. Arch. Gesamte Virusforsch. **44:**298–302.
6. **Hofmann, M. A., P. B. Sethna, and D. A. Brian.** 1990. Bovine coronavirus mRNA replication continues through persistent infection. J. Virol. **64:**4108–4114.
7. **Jeong, Y. S., and S. Makino.** 1992. Mechanism of coronavirus transcription: duration of primary transcription initiation activity and effect of subgenomic RNA transcription on RNA replication. J. Virol. **66:**3339–3346.
8. **Keck, J. G., B. G. Hogue, D. A. Brian, and M. M. C. Lai.** 1988. Temporal regulation of bovine coronavirus RNA synthesis. Virus Res. **9:**343–356.
9. **Lai, M. M. C., P. R. Brayton, R. C. Armen, C. D. Patton, C. Pugh, and S. A. Stohlman.** 1981. Mouse hepatitis virus A59: mRNA structure and genetic localization of the sequence divergence from hepatotropic strain MHV-3. J. Virol. **39:**823–834.
10. **Lai, M. M. C., C. D. Patton, R. S. Baric, and S. A. Stohlman.** 1983. Presence of leader sequences in the mRNA of mouse hepatitis virus. J. Virol. **46:**1027–1033.
11. **Leibowitz, J. L., K. C. Wilhelmsen, and C. W. Bond.** 1981. The virus-specific intracellular RNA species of two murine coronaviruses: MHV-A59 and MHV-JHM. Virology **114:**39–51.
12. **Lin, Y.-J., C.-L. Liao, and M. M. C. Lai.** 1994. Identification of the *cis*-acting signal for minus-strand RNA synthesis of a murine coronavirus: implication for the role of minus-strand RNA in RNA replication and transcription. J. Virol. **68:**8131–8140.
13. **Lu, X. T., A. C. Sims, and M. R. Denison.** 1998. Mouse hepatitis virus 3C-like protease cleaves a 22-kilodalton protein from the open reading frame 1a polyprotein in virus-infected cells and in vitro. J. Virol. **72:**2265–2271.
14. **Maeda, A., S. An, and S. Makino.** Importance of coronavirus negative-strand genomic RNA synthesis prior to subgenomic RNA transcription. Virus Res., in press.
15. **Makino, S., M. Joo, and J. K. Makino.** 1991. A system for study of coronavirus mRNA synthesis: a regulated, expressed subgenomic defective inter-

fering RNA results from intergenic site insertion. J. Virol. **65:**6031–6041.
16. **Makino, S., and M. M. C. Lai.** 1989. High-frequency leader sequence switching during coronavirus defective interfering RNA replication. J. Virol. **63:** 5285–5292.
17. **Makino, S., L. H. Soe, C.-K. Shieh, and M. M. C. Lai.** 1988. Discontinuous transcription generates heterogeneity at the leader fusion sites of coronavirus mRNA. J. Virol. **62:**3870–3873.
18. **Makino, S., K. Yokomori, and M. M. C. Lai.** 1990. Analysis of efficiently packaged defective interfering RNAs of murine coronavirus: localization of a possible RNA-packaging signal. J. Virol. **64:**6045–6053.
19. **Perlman, S., D. Ries, E. Bolger, L. J. Chang, and C. M. Stoltzfus.** 1986. MHV nucleocapsid synthesis in the presence of cycloheximide and accumulation of negative-strand MHV RNA. Virus Res. **6:**261–272.
20. **Sambrook, J., E. F. Fritsch, and T. Maniatis.** 1989. Molecular cloning: a laboratory manual, 2nd ed. Cold Spring Harbor Laboratory, Cold Spring Harbor, N.Y.
21. **Sawicki, S. G., and D. L. Sawicki.** 1986. Coronavirus minus-strand RNA synthesis and effect of cycloheximide on coronavirus RNA synthesis. J. Virol. **57:**328–334.
22. **Sawicki, S. G., and D. L. Sawicki.** 1990. Coronavirus transcription: subgenomic mouse hepatitis virus replicative intermediates function in RNA synthesis. J. Virol. **64:**1050–1056.
23. **Schaad, M. C., and R. S. Baric.** 1994. Genetics of mouse hepatitis virus transcription: evidence that subgenomic negative strands are functional templates. J. Virol. **68:**8169–8179.
24. **Sethna, P. B., M. A. Hofmann, and D. A. Brian.** 1991. Minus-strand copies of replicating coronavirus mRNAs contain antileaders. J. Virol. **65:**320–325.
25. **Sethna, P. B., S.-L. Hung, and D. A. Brian.** 1989. Coronavirus subgenomic minus-strand RNAs and the potential for mRNA replicons. Proc. Natl. Acad. Sci. USA **86:**5626–5630.
26. **Shieh, C.-K., L. H. Soe, S. Makino, M.-F. Chang, S A. Stohlman, and M. C. Lai.** 1987. The 5′-end sequences of the murine coronavirus genome: implications for multiple fusion sites in leader-primed transcription. Virology **156:**321–330.
27. **Spaan, W., H. Delius, M. Skinner, J. Armstrong, P. Rottier, S. Smeekens, B. A. M. van der Zeijst, and S. G. Siddell.** 1983. Coronavirus mRNA synthesis involves fusion of non-contiguous sequences. EMBO J. **2:**1939–1944.
28. **Stern, D. F., and S. I. T. Kennedy.** 1980. Coronavirus multiplication strategy. Identification and characterization of virus-specified RNA. J. Virol. **34:**665–674.
29. **van Dinten, L. C., J. A. den Boon, A. L. M. Wassenaar, W. J. M. Spaan, and E. J. Snijder.** 1997. An infectious arterivirus cDNA clone: identification of a replicase point mutation that abolishes discontinuous mRNA transcripton. Proc. Natl. Acad. Sci. USA **94:**991–996.
30. **Yokomori, K., L. R. Banner, and M. M. C. Lai.** 1992. Coronavirus mRNA transcription: UV light transcriptional mapping studies suggest an early requirement for a genomic-length template. J. Virol. **66:**4671–4678.
31. **Ziebuhr, J., J. Herold, and S. G. Siddell.** 1995. Characterization of a human coronavirus (strain 229E) 3C-like proteinase activity. J. Virol. **69:**4331–4338.
32. **Zinn, K., D. Dimaio, and T. Maniatis.** 1983. Identification of two distinct regulatory regions adjacent to the human beta-interferon gene. Cell **34:**865–879.